Published in final edited form as:
*Cancer Prev Res (Phila)*. 2009 July ; 2(7): . doi:10.1158/1940-6207.CAPR-08-0193.

# Topical Treatment with Black Raspberry Extract Reduces Cutaneous UVB-Induced Carcinogenesis and Inflammation

**F J. Duncan**[1,3], **Jason R. Martin**[1,3], **Brian C. Wulff**[1], **Gary D. Stoner**[2], **Kathleen L. Tober**[1], **Tatiana M. Oberyszyn**[1], **Donna F. Kusewitt**[4], and **Anne M. Van Buskirk**[3]

[1]Department of Pathology, The Ohio State University, Columbus, Ohio

[2]Department of Internal Medicine, The Ohio State University, Columbus, Ohio

[3]Department of Surgery, The Ohio State University, Columbus, Ohio

[4]Department of Carcinogenesis, University of Texas M.D. Anderson Cancer Center, Science Park Research Division, Smithville, Texas

## Abstract

Light in the UVB spectrum (280-320 nm) induces a number of changes in the epidermis and dermis of mice and humans, resulting in a robust inflammatory response. A standardized black raspberry extract (BRE) has been effective in reducing signaling pathways commonly initiated by inflammatory stimuli. In this study, we determined whether this extract could reduce cutaneous UVB-induced inflammation and carcinogenesis. In our carcinogenesis model, female SKH-1 hairless mice were exposed to one minimal erythemal dose of UVB thrice weekly on nonconsecutive days for 25 weeks. Immediately after each exposure, the mice were treated topically with either BRE dissolved in vehicle or with vehicle only. Beginning on week 19, mice treated with BRE had a significant reduction in tumor number and in average tumor size. This reduction correlated with a significant reduction in tumor-infiltrating $CD3^+foxp3^+$ regulatory T-cells. In the acute model, mice were exposed to a single minimal erythemal dose of UVB and treated topically with BRE or with vehicle. At 48 hours post-UVB exposure, topical BRE treatment significantly reduced edema, p53 protein levels, oxidative DNA damage, and neutrophil activation. The ability of topical BRE to reduce acute UVB-induced inflammation and to decrease tumor development in a long-term model provides compelling evidence to explore the clinical efficacy of BRE in the prevention of human skin cancers.

Exposure to UV light, particularly UVB (280-320 nm), initiates a robust inflammatory response (1) characterized by the influx and activation of innate immune cells, predominantly neutrophils and macrophages. Infiltration and activation of neutrophils is mediated via the release of chemokines and cytokines from the epidermis (2, 3). Macrophages and neutrophils are thought to be the main sources of the reactive oxygen species (ROS) that amplify the inflammatory response and thereby cause secondary DNA damage in keratinocytes (4, 5), although resident skin cells have also been shown to be a source of ROS production (6).



Requests for reprints: Tatiana M. Oberyszyn, The Ohio State University, 1645 Neil Avenue, 129 Hamilton Hall, Columbus, OH 43210. Phone: 614-293-9803; Fax: 614-293-9805; oberyszyn.1@osu.edu.
Current address for A.M. Van Buskirk: Medical and Scientific Affairs, Takeda Pharmaceuticals North America, Deerfield, IL.

**Note:** Supplementary data for this article are available at Cancer Prevention Research Online (http://cancerprevres.aacrjournals.org/).

**Disclosure of Potential Conflicts of Interest**: No potential conflicts of interest were disclosed.

The activation and infiltration of innate immune cells leads to the influx of cells of the adaptive immune system (7). We have previously shown that reducing $CD4^+$ T-cells in mice exacerbates the UVB-induced acute cutaneous inflammatory responses and increases tumor development (8). Others have shown that $CD8^+$ T-cells are critical in the inhibition of carcinogenesis by natural products (9). It is also known that regulatory T-cells ($CD3^+CD4^+foxp3^+$) have functional skin-homing markers (10). Understanding the interplay of these populations in UVB-induced carcinogenesis is crucial to understanding how tumors evade immune surveillance.

The most serious effect of chronic UVB exposure is the development of nonmelanoma skin cancer, the most frequently diagnosed cancer in the United States (11). Recent work has shown that there is a strong link between chronic inflammation and carcinogenesis in a number of organ systems (12, 13). This association holds true in the development of UVB-induced skin cancer as well (1, 14). The UVB-induced generation of ROS can produce oxidative DNA damage, resulting in the formation of 8-oxo-deoxyguanosine (8-oxo-dG) adducts (5). There has been increased interest in the last few years in the ability of natural compounds to combat inflammatory responses. One of the main classes of compounds investigated has been plant products that are high in antioxidants including anthocyanins and carotenoids. Studies from a number of laboratories have focused on testing a variety of standardized extracts made from black raspberries (15, 16). The ethanol/water extract of black raspberries (BRE) contains a number of powerful antioxidants, including cyanidin-3-*O*-glucoside, cyanidin 3-*O*-[2(G)-xylosylrutinoside], and cyanidin 3-*O*-rutinoside (17, 18). These molecules are not only effective antioxidants but are also able to affect signaling pathways activated in inflammatory responses (19). The promising findings regarding the ability of natural products to inhibit the inflammatory process have carried over to cancer studies in a variety of organs including the oral cavity and the skin. Natural compounds, such as tea polyphenols, fruit extracts, and spices, have shown promise *in vivo* in reducing carcinogenesis in the skin (reviewed in ref. 20). In *in vitro* models, BRE has been found to induce apoptosis in a number of transformed cell lines, but had no effect upon the growth of normal cells (21).

The present study was designed to determine if topical BRE treatment is effective at reducing carcinogenesis and the inflammatory response in murine skin following UVB exposure. We have shown that topical treatment with BRE immediately following UVB exposure significantly reduced UVB-induced tumor formation and progression. We have also shown that treatment with BRE reduced the edematous response, neutrophil activation, and oxidative DNA damage, indicating that BRE was a strong inhibitor of the inflammatory response initiated by UVB exposure. These data suggest that topical application of BRE following UVB exposure may be a beneficial treatment for the prevention of UVB-mediated inflammation as well as tumor development.

## Materials and Methods

### Standardized BRE preparation

Standardized BRE was prepared as previously reported (22). Briefly, Jewel varietal black raspberries were grown at the Stokes Raspberry Farm (Wilmington, OH), harvested, washed, and frozen according to previously determined protocols (23). The berries were assayed by Covance Laboratories to determine levels of pesticides/herbicides/fungicides, which were found to be negligible. Berries were then freeze-dried and shipped frozen to the laboratory of Dr. S. Hecht at the University of Minnesota where the extract was prepared as previously reported (17, 22). The most prevalent peaks in a high-performance liquid chromatograph of the ethanol/water (80:20) extract of black raspberries are anthocyanins, and make up 5% to 10% of the dry berry weight (24). Anthocyanins, particularly

cyanidin-3-*O*-glucoside, cyanidin-3-*O*-rutinoside, and cyanidin-3-*O*-xylosylrutinoside have been shown to be effective anticancer agents in a number of model systems, both *in vitro* and *in vivo* (17, 18, 25–35). These extracts have been shown to be rapidly uptaken and pass rapidly through tissues, which, coupled with the post-exposure application and low dosage, makes the likelihood of accumulation in the skin and the production of a sun-blocking effect very low (36).

## Animal treatment

Six-week-old to 8-week-old female SKH-1 hairless mice (Charles River Laboratories) were housed in a vivarium at The Ohio State University according to protocols established by the American Association for Accreditation of Laboratory Animal Care. Mice were housed at constant temperature and humidity levels. Food and water containing the antibiotic Baytril (Bayer HealthCare, LLC) was provided *ad libitum*. All procedures done were approved by the Institutional Laboratory Animal Care and Use Committee. All mice treated with extract received 500 μg of BRE dissolved in 100 μL of vehicle (KY Jelly; McNeil Consumer & Specialty Pharmaceuticals). This dosage was decided on after preliminary dose-response experiments testing the efficacy of BRE concentrations ranging from 100 μg to 1 mg, which showed that the 500 μg dose was optimal for the inhibition of acute UVB-induced inflammatory responses in the skin.

**Carcinogenesis model—**Mice ($n$ = 10 per group) were exposed to one minimal erythemal dose of UVB, which was previously established in our lab as 2,240 J/m$^2$ (1). UVB levels were measured using a UVX radiometer (UVP, Inc.). UVB light was generated by a bank of Philips FS40UVB lamps (American Ultraviolet Company) covered by Kodacel filters (Eastman Kodak) to block UVC wavelengths. Groups of mice were exposed to UVB in large rat cages. The positions of these cages were rotated on a weekly basis to standardize exposure conditions. Mice received one minimal erythemal dose of UVB followed immediately by topical application of 500 μg of BRE dissolved in 100 μL vehicle or 100 μL vehicle alone thrice weekly on nonconsecutive days for 25 weeks. Several laboratories have shown that anthocyanins are readily absorbed and excreted by the body, with peak levels of anthocyanin excretion occurring at 4 to 8 h (37–39). This rapid absorption and processing and the gap between treatments reduced the risk of sunscreen effects. BRE was placed in the middle of the dorsum of the mouse and manually gently rubbed into the dorsal skin by glove-wearing personnel immediately after UVB exposure. All mice were treated within 2 min of the cessation of UVB exposure. Mice were sacrificed at 48 h following the final UVB exposure, which is the peak UVB-induced inflammatory time point, and topical treatment. Nonirradiated age-matched control mice were treated topically with vehicle or BRE. Beginning on week 11, the length and width of each tumor <1 mm in each direction were measured using digital calipers; these measurements were used to calculate tumor area. At harvest, tumor samples were fixed in 10% neutral buffered formalin or placed in optimal cutting temperature compound (Sakura Finetek, Torrence, CA) for further processing and histologic analysis. The remaining dorsal skin was snap-frozen in liquid nitrogen for protein isolation.

**Acute inflammation model—**Mice ($n$ = 6 per group) were exposed to one minimal erythemal dose of UVB (2240 J/m$^2$), followed immediately by topical application of 500 μg of BRE dissolved in 100 μL vehicle or 100 μL vehicle alone as described above. Mice were sacrificed 48 h following UVB exposure. This time point was chosen because it represents the height of the acute UVB-induced cutaneous inflammatory response. Nonirradiated age-matched control mice were treated topically with vehicle or BRE. At harvest, edema, as determined by skin fold thickness measurements, was recorded and dorsal skin samples were fixed in 10% neutral buffered formalin or placed in optimal cutting temperature

compound (Tissue-Tek, Sakura Finetek) for further processing and histologic analysis. Skin punches were snap-frozen in liquid nitrogen for subsequent determination of myeloperoxidase activity. The remaining dorsal skin was snap-frozen in liquid nitrogen for protein isolation.

### Immunofluorescence staining of tumors

At the time of sacrifice, tumors were removed and placed into optimal cutting temperature compound before being frozen on dry ice. To determine the presence of specific subpopulations of T cells, 5-μm sections were cut and stained with antibodies recognizing CD3, CD4 (PharMingen), or foxp3 (eBioscience). A total of 15 tumors per group were analyzed. Sections were incubated with primary antibody overnight at 4°C before washing to remove the primary antibody. The sections were then incubated with the appropriate Alexa Fluor conjugated secondary antibody (Invitrogen). Sections were then incubated with the final primary and secondary antibodies at room temperature (1 h) before being counterstained with 4′,6-diamidino-2-phenylindole (Sigma Aldrich) and coverslipped using ProLong Gold (Invitrogen). For T-cell measurements, the number of positive cells within tumor margins was counted for each animal and the mean was determined for each group.

### Edema measurement

Dorsal skin edema induced by acute UVB exposure was measured by determining skin fold thickness at harvest using digital calipers. Data shown are the mean ± SD of each group.

### Myeloperoxidase assay

The level of myeloperoxidase was measured as previously described (40). Briefly, a 10-mm skin biopsy was snap-frozen at harvest and stored at −80°C. Biopsies were incubated on ice in phosphate buffer containing hexadecyltrimethylammonium bromide. Tissue samples were homogenized and then underwent three cycles of sonication and freeze-thawing. Cellular debris was removed by centrifugation. The myeloperoxidase levels of the supernatants were then analyzed spectrophotometrically. Results are reported as fold increase compared with matched control samples from mice not exposed to UVB. The rate of $H_2O_2$ consumption was measured spectrophotometrically over a 5-min period.

### Immunohistochemical staining

Skin samples from the inflammation model were removed and fixed in 10% neutral buffered formalin, embedded in paraffin, and sectioned at 5 μm. Sections were stained for Ly6G (a neutrophil marker) to identify infiltrating neutrophils as reported previously (40). Briefly, sections were rehydrated and blocked using 10% normal goat serum (Vector Laboratories) for 1 h. The slides were then incubated overnight at 4°C with the primary antibody (monoclonal rat anti-mouse Ly6G; PharMingen). The next day, the slides were washed and incubated with the biotinylated anti-rat secondary antibody (Vector Laboratories) for 30 min at room temperature. Slides were then incubated with an avidin/horseradish peroxidase complex (ABC Elite, Vector Laboratories) for 30 min. The slides were developed using a 3,3′-diaminobenzidine kit (Vector Laboratories) and counterstained with hematoxylin before being dehydrated in a series of ethanol washes ending in Clear-Rite. Slides were then coverslipped. To determine the number of neutrophils infiltrating into the dermis, the mean number of neutrophils per 10 fields per 5-μm section per mouse at 600× magnification was calculated.

p53 levels in keratinocytes were measured using a similar method. Dorsal skin was harvested 48 h after UVB exposure and treatment with vehicle or 500 μg of BRE. Paraffin-embedded sections were cut and treated with the Mouse-on-Mouse kit (Vector

Laboratories), then stained with anti-rabbit p53 (Leica Microsystems). Link-Label (Biogenex) was used to amplify the signal and the slides were developed using the 3,3′-diaminobenzidine system (Vector Laboratories). The number of p53-positive cells per 10 fields per 5-μm section at 600× magnification per mouse in the epidermis was counted and averaged.

### 8-Oxo-dG adduct detection

To identify differences in ROS-induced DNA damage, flash-frozen dorsal epidermis was scraped from whole skin and used to isolate DNA. Briefly, frozen scraped epidermis was incubated for 4 h at 45°C in solubilization buffer (10% SDS, 50 mmol/L EDTA, 100 mmol/L Tris, 100 mmol/L NaCl, and 200 μg/mL proteinase K). After cooling to room temperature, 200 μL of a 4.21 mol/L NaCl, 0.63 mol/L KCl, 10 mmol/L Tris solution was added and incubated at 4°C for 30 min to precipitate proteins. Samples were centrifuged at 13,000 × *g* for 10 min and supernatant removed for DNA precipitation. DNA was precipitated with 100% ethanol at 4°C overnight. DNA was pelleted by centrifugation at 2,000 × *g* for 7 min and washed with 80% ethanol thrice. Washed DNA was resuspended in 0.4 mol/L NaOH/10 mmol/L EDTA and the concentration was determined spectrophotometrically. Equal amounts of DNA from each animal in the different treatment groups were pooled for 8-oxo-dG Southwestern blots.

Southwestern immunoblots were done as previously reported (5). Briefly, 5 μg of epidermal DNA was loaded onto a nitrocellulose membrane and dried for 1 h before being blocked with 5% bovine serum albumin in TBST (TBS + 0.1% v/v Tween 20; Fisher Scientific). The blot was then incubated overnight with the 8-oxo-dG primary antibody (Genox Corporation). After overnight incubation, the blot was washed and incubated with a goat anti-mouse horseradish peroxidase–conjugated secondary antibody (Thermo Fisher Scientific) for 45 min at room temperature. The blot was washed and incubated with West Femto Supersignal chemiluminescent reagent (Bio-Rad) and exposed to Kodak Biomax MR Film (Kodak). It was then incubated in 4′,6-diamidino-2-phenylindole and scanned with a Pharos FX scanner (Bio-Rad) to normalize for DNA adhesion. The ratio of 8-oxo-dG dot intensity to 4′,6-diamidino-2-phenylindole dot intensity was determined using ImageJ version 1.28b.[5]

### Statistical analysis

**Chronic UVB exposure—**After consultation with a biostatistician, we determined that the Mann-Whitney test was the most appropriate for our data. The tumor number and area data was analyzed using Minitab. $P < 0.05$ was considered significant and $P < 0.01$was considered highly significant. To determine statistical significance for the large tumor data, we used Student's two-tailed *t* test.

**Acute UVB exposure—**We did statistical analyses using Excel (Microsoft Corporation). After consultation with a biostatistician, Student's two-tailed *t* test was used to determine statistical significance. $P < 0.05$ was considered significant and $P < 0.01$was considered highly significant.

[5] http://rsbweb.nih.gov/ij/

## Results

### BRE treatment significantly reduced UVB-induced carcinogenesis

Tumor measurements were collected beginning on week 11. As can be seen in Fig. 1A, by 25 weeks, vehicle-treated mice developed, on average, 30 tumors / mouse (±3.1). In contrast, treatment with BRE significantly reduced the total number of tumors on the dorsum of UVB-exposed mice to 17 tumors / mouse (±1.9; $P = 0.001$). Thus, topical treatment with BRE following UVB exposure reduced the number of tumors that developed in response to chronic UVB exposure.

### BRE treatment decreased tumor size and inhibited tumor progression

BRE treatment also significantly reduced the size of the tumors per mouse, from a mean of 30.2 $mm^2$ in vehicle-treated mice to 10.1 $mm^2$ in BRE-treated mice ($P = 0.004$; Fig. 1B). The number of tumors measuring >10 $mm^2$ in area were counted and averaged for each group. BRE treatment reduced the average number of large tumors at week 25 from 6.9 to 1.6 ($P = 0.004$; Fig. 1C). Thus, BRE treatment significantly retarded the growth of UVB-induced tumors.

### Tumors from mice treated with BRE contain significantly fewer $CD3^+foxp3^+$ T-cells

To determine how BRE was able to alter tumor progression, we explored how BRE affected T-cell infiltration into tumors. BRE reduced the number of tumor-infiltrating $CD4^+$ T-cells within tumors from a mean of 206 in mice treated with vehicle to 77 in mice treated with BRE ($P \ll 0.001$; Fig. 2C). Representative micrographs of tumors from vehicle-treated (A) and BRE-treated (B) mice are shown in Fig. 2. Analysis of the number of $CD3^+foxp3^+$ T-cells within the tumors showed a significant reduction, down from 10 in vehicle-treated mice to 2.2 in BRE-treated mice ($P = 0.01$; Fig. 3C). Representative micrographs of tumors from vehicle-treated (A) and BRE-treated (B) mice are shown in Fig. 3. There was no significant difference in the number of infiltrating $CD8^+$ T-cells in any tumor (data not shown).

### BRE treatment reduced acute UVB-induced edema

To determine if the observed antitumor effects of BRE treatment were being mediated at least in part by a decreased inflammatory response, we examined the effects of BRE treatment on the acute UVB-induced inflammation. The most visible responses to acute UVB exposure are erythema and edema, which can be used as an indicator of the severity of the inflammatory response. All mice were sacrificed 48 hours post-UVB exposure, at the peak of the inflammatory response in the skin. Post-exposure treatment with 500 μg of BRE significantly reduced UVB-induced edema (determined via single fold dorsal skin thickness) at 48 hours following UVB exposure ($P = 0.001$, compared with UVB-exposed vehicle-treated controls; Fig. 4A).

### BRE treatment reduced neutrophil activation, but did not reduce neutrophil infiltration

Although topical BRE treatment decreased edema, topical BRE treatment did not reduce dermal neutrophil numbers compared with vehicle (Supplemental data Fig. S1). Mice were grouped as follows: mice unexposed to UVB and treated with vehicle (no UV vehicle), mice unexposed to UVB and treated with BRE (no UV BRE), mice exposed to UVB and treated with vehicle (UV vehicle), and mice exposed to UVB and treated with BRE (UV BRE). BRE treatment did significantly reduce neutrophil activation as measured by myeloperoxidase levels ($P = 0.03$, compared with vehicle; Fig. 4B). The ability of BRE to decrease myeloperoxidase without affecting neutrophil homing suggests that BRE selectively inhibits neutrophil activation.

### BRE treatment decreased p53 expression

To estimate the overall DNA damage response in BRE-treated and vehicle-treated skin, dorsal skin was stained for p53 and the mean number of keratinocytes with positive nuclei per 600× magnification field was determined. Treatment with BRE significantly reduced the number of UVB-induced p53-postive cells ($P = 0.002$, compared with vehicle; Fig. 5), suggesting less overall cellular damage.

### BRE treatment significantly reduced the levels of indirect DNA adducts but not direct adducts

To assess the level of indirect DNA damage induced by ROS formed during the inflammatory response to UVB, we did a Southwestern immunoblot for 8-oxo-dG on DNA isolated from the epidermis (Fig. 6A). The densitometry data (Fig. 6B) show that BRE treatment significantly ($P = 0.04$, compared with vehicle controls) reduced the levels of 8-oxo-dG adducts in the epidermis of mice exposed to UVB down to those seen in mice that had not been exposed to UVB. Immunohistochemical staining of dorsal skin sections for the presence of cyclobutane pyrimidine dimers (CPD), a measure of direct UV-induced DNA damage (Fig. 6C), show that treatment with BRE did not significantly reduce the formation of direct DNA adducts.

## Discussion

Recent studies have explored the use of natural compounds in the prevention of several types of cancer, including SCC of the skin. For example, myricetin, a phytochemical found in nuts and dark-pigmented fruits, was shown to significantly reduce tumor formation in mice chronically exposed to UVB light (41). Other dietary botanicals including apigenin, curcumin, resveratrol, and green tea have been shown to reduce the deleterious effects of UVB exposure (20). Anthocyanins, found in red, blue, and purple fruits and vegetables, have also been studied for their chemopreventive properties. Ohio-grown black raspberries and extracts made from these berries, which have high levels of anthocyanins and other compounds, have been shown in an animal model to be efficacious in preventing esophageal cancer (42). Ongoing studies are determining their efficacy in both colon and oral cancers (24, 43). To date, however, no *in vivo* studies have examined the efficacy of a standardized BRE in the prevention of cutaneous UVB-induced damage or tumor development.

Many groups have shown that inhibition of inflammation leads to a reduction in carcinogenesis (1, 12, 14, 40). We have previously shown that topical application of the anti-inflammatory drug celecoxib reduced both acute UVB-mediated inflammation and chronic UVB-mediated tumor formation. We have also found that agents increasing UVB-induced inflammation lead to an increase in tumors with an area of >10 $mm^2$, which were of a high malignant grade (1, 14). These studies supported the link between UVB-induced inflammation and skin cancer development. Natural products, such as (−)-epigallocatechin-3-gallate, a green tea polyphenol, have also been shown to reduce acute inflammation and inhibit UVB-induced carcinogenesis (44). Our present data shows the ability of BRE, a natural product, to inhibit several hallmarks of UVB-mediated inflammation including the production of DNA-damaging ROS in the skin.

Exposure to light in the UVB wavelength (280-320 nm) produces both direct and indirect DNA damage. Direct DNA damage from UVB absorption results in the formation of CPD (45–47). Indirect DNA damage, including signature DNA adducts such as 8-oxo-dG, results from the activity of ROS generated by keratinocytes and infiltrating inflammatory cells, especially neutrophils, during the inflammatory response to UVB (5, 48). These ROS can damage keratinocytes, which induces the production of more proinflammatory cytokines and

chemokines, thus amplifying the inflammatory response (49). We have previously shown that the inhibition of UVB-induced neutrophil infiltration and especially neutrophil activation can lead to decreased inflammation and tumor development (1). Our current data showed that whereas BRE treatment had no effect on neutrophil infiltration, it significantly reduced myeloperoxidase and $H_2O_2$ levels (Figs. 4B and 6B), thus decreasing ROS levels in the skin, and ultimately, oxidative DNA damage.

Epidermal keratinocytes have mechanisms to repair both direct and indirect damage initiated by UVB exposure. One of the ways they accomplish this is by p53 production and activation, which halts the cell cycle and allows DNA repair mechanisms to correct the CPD and 8-oxo-dG adducts, or induce apoptosis if the damage is beyond repair (50). p53 stabilization, indicated by nuclear immunoreactivity, has previously been used as an indicator of overall levels of DNA damage (8, 51). The present study found that topical application of BRE following UVB exposure was able to reduce the number of p53-positive epidermal cells, indicating less overall damage in the epidermis. Our studies determined that topical BRE application following exposure to UVB did not decrease the formation of direct DNA damage adducts CPDs, demonstrating that BRE was not acting as a sunscreen. However, similar to other topical inhibitors of inflammation (1, 52), BRE did significantly inhibit the formation of the ROS-induced 8-oxo-dG adducts. We cannot discern from our data whether the reduction in 8-oxo-dG adducts was attributable to the inhibition of initial adduct formation or enhancement of DNA repair. Ongoing studies are further examining this question. However, our findings that BRE treatment significantly decreased levels of the potent ROS $H_2O_2$, suggest that BRE treatment reduced ROS levels in the epidermis and dermis of the skin, thus decreasing initial ROS-mediated DNA damage. Regardless of the mechanism of reduction of 8-oxo-dG formation, the formation of fewer oxidative DNA adducts would ultimately result in decreased carcinogenesis.

In addition to decreasing inflammation and oxidative DNA damage, another possible mechanism by which BRE may be altering UVB-mediated tumor development and progression is by altering the infiltration of the adaptive immune cells. It is now known that the influx of regulatory T-cells is one mechanism by which transformed cells can evade immune surveillance (53). Yang et al. was one of the first to report that treatment with resveratrol, a natural product derived from grape skins, reduced the number of regulatory T-cells in the spleens of mice who had been injected with lymphoma or colon cancer cells (54). It has also been shown in mice that chronic UVB exposure leads to an increase in regulatory T-cells (55) and that this cell type express functional skin-homing receptors (10). Although there have been no previous reports of anthrocyanins having an effect on the adaptive immune response, our data suggests that Tcells with a regulatory phenotype are reduced in the tumors isolated from BRE-treated mice (Fig. 3C). The reduction in putative regulatory T-cells suggests a possible mechanism for the observed reduction in the number of large tumors in BRE-treated skin (Fig. 1C). It is important to note that although we did see a decrease in $CD4^+$ cells within tumors isolated from BRE-treated mice, we did see did not see a reduction in $CD8^+$ T-cells in any of the tumors (data not shown). The observed reduction in the number of cells with an immunosuppressive regulatory phenotype may then allow $CD4^+$ and $CD8^+$ effector cells to aid the innate and adaptive immune system to reject tumor cells. Although our data is suggestive, we did not isolate the cells and test their ability to suppress immune responses. Neither did we remove these cells from the mice to determine what effect that would have on tumor development. These types of future studies will provide further confirmation of the importance of immune cell regulation in the skin by BRE treatment. Completion of these preclinical studies will provide valuable information leading to more effective skin cancer prevention strategies.

## Supplementary Material

Refer to Web version on PubMed Central for supplementary material.

## Acknowledgments

We thank Dr. Stephen Hecht of the University of Minnesota Cancer Center for providing the black raspberry extract.

**Grant support:** National Center for Complementary and Alternative Medicine grant no. R21 AT 3959 (T.M. Oberyszyn) and Fellowship F31 AT03996 (F J. Duncan), and National Cancer Institute grant no. CA103180 (G.D. Stoner). The contents of this article are solely the responsibility of the authors and do not necessarily represent the official views of the National Center for Complementary and Alternative Medicine or the NIH.

## References

1. Wilgus TA, Koki AT, Zweifel BS, Kusewitt DF, Rubal PA, Oberyszyn TM. Inhibition of cutaneous ultraviolet light B-mediated inflammation and tumor formation with topical celecoxib treatment. Mol Carcinog. 2003; 38:49–58. [PubMed: 14502644]
2. Hawk JL, Murphy GM, Holden CA. The presence of neutrophils in human cutaneous ultraviolet-B inflammation. Br J Dermatol. 1988; 118:27–30. [PubMed: 3342174]
3. Eberlein-Konig B, Jager C, Przybilla B. Ultraviolet B radiation-induced production of interleukin 1α and interleukin 6 in a human squamous carcinoma cell line is wavelength-dependent and can be inhibited by pharmacological agents. Br J Dermatol. 1998; 139:415–21. [PubMed: 9767285]
4. Komatsu J, Koyama H, Maeda N, Aratani Y. Earlier onset of neutrophil-mediated inflammation in the ultraviolet-exposed skin of mice deficient in myeloperoxidase and NADPH oxidase. Inflamm Res. 2006; 55:200–6. [PubMed: 16830107]
5. Wulff BC, Schick JS, Thomas-Ahner JM, Kusewitt DF, Yarosh DB, Oberyszyn TM. Topical treatment with OGG1 enzyme affects UVB-induced skin carcinogenesis. Photochem Photobiol. 2008; 84:317–21. [PubMed: 18086242]
6. Chang H, Oehrl W, Elsner P, Thiele JJ. The role of $H_2O_2$ as a mediator of UVB-induced apoptosis in keratinocytes. Free Radic Res. 2003; 37:655–63. [PubMed: 12868492]
7. Terui T, Takahashi K, Funayama M, et al. Occurrence of neutrophils and activated Th1 cells in UVB-induced erythema. Acta Derm Venereol. 2001; 81:8–13. [PubMed: 11411937]
8. Hatton JL, Parent A, Tober KL, et al. Depletion of CD4+ cells exacerbates the cutaneous response to acute and chronic UVB exposure. J Invest Dermatol. 2007; 127:1507–15. [PubMed: 17363918]
9. Mantena SK, Meeran SM, Elmets CA, Katiyar SK. Orally administered green tea polyphenols prevent ultraviolet radiation-induced skin cancer in mice through activation of cytotoxic Tcells and inhibition of angiogenesis in tumors. J Nutr. 2005; 135:2871–7. [PubMed: 16317135]
10. Hirahara K, Liu L, Clark RA, Yamanaka K, Fuhlbrigge RC, Kupper TS. The majority of human peripheral blood CD4+CD25highFoxp3+ regulatory T cells bear functional skin-homing receptors. J Immunol. 2006; 177:4488–94. [PubMed: 16982885]
11. Gloster HM Jr, Brodland DG. The epidemiology of skin cancer. Dermatol Surg. 1996; 22:217–26. [PubMed: 8599733]
12. Greten FR, Eckmann L, Greten TF, et al. IKKβ links inflammation and tumorigenesis in a mouse model of colitis-associated cancer. Cell. 2004; 118:285–96. [PubMed: 15294155]
13. Jung YJ, Isaacs JS, Lee S, Trepel J, Neckers L. IL-1β-mediated up-regulation of HIF-1α via an NFκB/COX-2 pathway identifies HIF-1 as a critical link between inflammation and oncogenesis. FAS-EB J. 2003; 17:2115–7.
14. Duncan FJ, Wulff BC, Tober KL, et al. Clinically relevant immunosuppressants influence UVB-induced tumor size through effects on inflammation and angiogenesis. Am J Transplant. 2007; 7:2693–703. [PubMed: 17941958]
15. Harris GK, Gupta A, Nines RG, et al. Effects of lyophilized black raspberries on azoxymethane-induced colon cancer and 8-hydroxy-2′-deoxyguanosine levels in the Fischer 344 rat. Nutr Cancer. 2001; 40:125–33. [PubMed: 11962247]

16. Rodrigo KA, Rawal Y, Renner RJ, et al. Suppression of the tumorigenic phenotype in human oral squamous cell carcinoma cells by an ethanol extract derived from freeze-dried black raspberries. Nutr Cancer. 2006; 54:58–68. [PubMed: 16800773]

17. Hecht SS, Huang C, Stoner GD, et al. Identification of cyanidin glycosides as constituents of freeze-dried black raspberries which inhibit anti-benzo[a] pyrene-7,8-diol-9,10-epoxide induced NFκB and AP-1 activity. Carcinogenesis. 2006; 27:1617–26. [PubMed: 16522666]

18. Tulio AZ Jr, Reese RN, Wyzgoski FJ, et al. Cyanidin 3-rutinoside and cyanidin 3-xylosylrutinoside as primary phenolic antioxidants in black raspberry. J Agric Food Chem. 2008; 56:1880–8. [PubMed: 18290621]

19. Chen T, Hwang H, Rose ME, Nines RG, Stoner GD. Chemopreventive properties of black raspberries in N-nitrosomethylbenzylamine-induced rat esophageal tumorigenesis: down-regulation of cyclooxygenase-2, inducible nitric oxide synthase, and c-Jun. Cancer Res. 2006; 66:2853–9. [PubMed: 16510608]

20. Baliga MS, Katiyar SK. Chemoprevention of photocarcinogenesis by selected dietary botanicals. Photochem Photobiol Sci. 2006; 5:243–53. [PubMed: 16465310]

21. Han C, Ding H, Casto B, Stoner GD, D'Ambrosio SM. Inhibition of the growth of premalignant and malignant human oral cell lines by extracts and components of black raspberries. Nutr Cancer. 2005; 51:207–17. [PubMed: 15860443]

22. Wang LS, Hecht SS, Carmella SG, et al. Anthocyanins in black raspberries prevent esophageal tumors in rats. Cancer Prev Res (Phila Pa). 2009; 2:84–93.

23. Stoner GD, Kresty LA, Carlton PS, Siglin JC, Morse MA. Isothiocyanates and freeze-dried strawberries as inhibitors of esophageal cancer. Toxicol Sci. 1999; 52:95–100. [PubMed: 10630596]

24. Stoner GD, Wang LS, Casto BC. Laboratory and clinical studies of cancer chemoprevention by antioxidants in berries. Carcinogenesis. 2008; 29:1665–74. [PubMed: 18544560]

25. Feng R, Ni HM, Wang SY, et al. Cyanidin-3-rutinoside, a natural polyphenol antioxidant, selectively kills leukemic cells by induction of oxidative stress. J Biol Chem. 2007; 282:13468–76. [PubMed: 17360708]

26. Fimognari C, Berti F, Nusse M, Cantelli-Forti G, Hrelia P. Induction of apoptosis in two human leukemia cell lines as well as differentiation in human promyelocytic cells by cyanidin-3-*O*-β-glucopyranoside. Biochem Pharmacol. 2004; 67:2047–56. [PubMed: 15135302]

27. Hou DX, Kai K, Li JJ, et al. Anthocyanidins inhibit activator protein 1 activity and cell transformation: structure-activity relationship and molecular mechanisms. Carcinogenesis. 2004; 25:29–36. [PubMed: 14514663]

28. Malik M, Zhao C, Schoene N, Guisti MM, Moyer MP, Magnuson BA. Anthocyanin-rich extract from *Aronia meloncarpa* E induces a cell cycle block in colon cancer but not normal colonic cells. Nutr Cancer. 2003; 46:186–96. [PubMed: 14690795]

29. Seeram NP, Adams LS, Zhang Y, et al. Blackberry, black raspberry, blueberry, cranberry, red raspberry, and strawberry extracts inhibit growth and stimulate apoptosis of human cancer cells *in vitro*. J Agric Food Chem. 2006; 54:9329–39. [PubMed: 17147415]

30. Seeram NP, Zhang Y, Nair MG. Inhibition of proliferation of human cancer cells and cyclooxygenase enzymes by anthocyanidins and catechins. Nutr Cancer. 2003; 46:101–6. [PubMed: 12925310]

31. Shih PH, Yeh CT, Yen GC. Effects of anthocyanidin on the inhibition of proliferation and induction of apoptosis in human gastric adenocarcinoma cells. Food Chem Toxicol. 2005; 43:1557–66. [PubMed: 15964118]

32. Tarozzi A, Marchesi A, Hrelia S, et al. Protective effects of cyanidin-3-*O*-β-glucopyranoside against UVA-induced oxidative stress in human keratinocytes. Photochem Photobiol. 2005; 81:623–9. [PubMed: 15701043]

33. Tsuda T, Horio F, Kato Y, Osawa T. Cyanidin 3-*O*-β-d-glucoside attenuates the hepatic ischemia-reperfusion injury through a decrease in the neutrophil chemoattractant production in rats. J Nutr Sci Vitaminol (Tokyo). 2002; 48:134–41. [PubMed: 12171434]

34. Yeh CT, Yen GC. Induction of apoptosis by the anthocyanidins through regulation of Bcl-2 gene and activation of c-Jun N-terminal kinase cascade in hepatoma cells. J Agric Food Chem. 2005; 53:1740–9. [PubMed: 15740068]
35. Zhang Y, Vareed SK, Nair MG. Human tumor cell growth inhibition by nontoxic anthocyanidins, the pigments in fruits and vegetables. Life Sci. 2005; 76:1465–72. [PubMed: 15680311]
36. Shumway BS, Kresty LA, Larsen PE, et al. Effects of a topically applied bioadhesive berry gel on loss of heterozygosity indices in premalignant oral lesions. Clin Cancer Res. 2008; 14:2421–30. [PubMed: 18413833]
37. McGhie TK, Ainge GD, Barnett LE, Cooney JM, Jensen DJ. Anthocyanin glycosides from berry fruit are absorbed and excreted unmetabolized by both humans and rats. J Agric Food Chem. 2003; 51:4539–48. [PubMed: 14705874]
38. Wu X, Pittman HE III, Prior RL. Fate of anthocyanins and antioxidant capacity in contents of the gastrointestinal tract of weanling pigs following black raspberry consumption. J Agric Food Chem. 2006; 54:583–9. [PubMed: 16417325]
39. Tian Q, Giusti MM, Stoner GD, Schwartz SJ. Urinary excretion of black raspberry (*Rubus occidentalis*) anthocyanins and their metabolites. J Agric Food Chem. 2006; 54:1467–72. [PubMed: 16478275]
40. Wilgus TA, Parrett ML, Ross MS, Tober KL, Robertson FM, Oberyszyn TM. Inhibition of ultraviolet light B-induced cutaneous inflammation by a specific cyclooxygenase-2 inhibitor. Adv Exp Med Biol. 2002; 507:85–92. [PubMed: 12664569]
41. Jung SK, Lee KW, Byun S, et al. Myricetin suppresses UVB-induced skin cancer by targeting Fyn. Cancer Res. 2008; 68:6021–9. [PubMed: 18632659]
42. Wang LS, Stoner GD. Anthocyanins and their role in cancer prevention. Cancer Lett. 2008; 269:281–90. [PubMed: 18571839]
43. Mallery SR, Zwick JC, Pei P, et al. Topical application of a bioadhesive black raspberry gel modulates gene expression and reduces cyclooxygenase 2 protein in human premalignant oral lesions. Cancer Res. 2008; 68:4945–57. [PubMed: 18559542]
44. Mantena SK, Roy AM, Katiyar SK. Epigallocatechin-3-gallate inhibits photocarcinogenesis through inhibition of angiogenic factors and activation of CD8+ Tcells in tumors. Photochem Photobiol. 2005; 81:1174–9. [PubMed: 15938647]
45. Besaratinia A, Synold TW, Chen HH, et al. DNA lesions induced by UV A1 and B radiation in human cells: comparative analyses in the overall genome and in the p53 tumor suppressor gene. Proc Natl Acad Sci U S A. 2005; 102:10058–63. [PubMed: 16009942]
46. De Haes P, Garmyn M, Verstuyf A, et al. 1,25-Dihydroxyvitamin $D_3$ and analogues protect primary human keratinocytes against UVB-induced DNA damage. J Photochem Photobiol B. 2005; 78:141–8. [PubMed: 15664501]
47. Belletti S, Uggeri J, Gatti R, Govoni P, Guizzardi S. Polydeoxyribonucleotide promotes cyclobutane pyrimidine dimer repair in UVB-exposed dermal fibroblasts. Photodermatol Photoimmunol Photomed. 2007; 23:242–9. [PubMed: 17986061]
48. van der Kemp PA, Blais JC, Bazin M, Boiteux S, Santus R. Ultraviolet-B-induced inactivation of human OGG1, the repair enzyme for removal of 8-oxoguanine in DNA. Photochem Photobiol. 2002; 76:640–8. [PubMed: 12511044]
49. Soter NA. Acute effects of ultraviolet radiation on the skin. Semin Dermatol. 1990; 9:11–5. [PubMed: 2203437]
50. Mrass P, Rendl M, Mildner M, et al. Retinoic acid increases the expression of p53 and proapoptotic caspases and sensitizes keratinocytes to apoptosis: a possible explanation for tumor preventive action of retinoids. Cancer Res. 2004; 64:6542–8. [PubMed: 15374966]
51. Selivanova G. p53 induction as an indicator of DNA damage. Methods Mol Biol. 2002; 203:279–88. [PubMed: 12073449]
52. Tober KL, Wilgus TA, Kusewitt DF, Thomas-Ahner JM, Maruyama T, Oberyszyn TM. Importance of the EP(1) receptor in cutaneous UVB-induced inflammation and tumor development. J Invest Dermatol. 2006; 126:205–11. [PubMed: 16417238]

53. Heier I, Hofgaard PO, Brandtzaeg P, Jahnsen FL, Karlsson M. Depletion of CD4+ CD25+ regulatory Tcells inhibits local tumour growth in a mouse model of B cell lymphoma. Clin Exp Immunol. 2008; 152:381–7. [PubMed: 18341610]

54. Yang Y, Paik JH, Cho D, Cho JA, Kim CW. Resveratrol induces the suppression of tumor-derived CD4+CD25+ regulatory T cells. Int Immunopharmacol. 2008; 8:542–7. [PubMed: 18328445]

55. Loser K, Scherer A, Krummen MB, et al. An important role of CD80/CD86-CTLA-4 signaling during photocarcinogenesis in mice. J Immunol. 2005; 174:5298–305. [PubMed: 15843526]

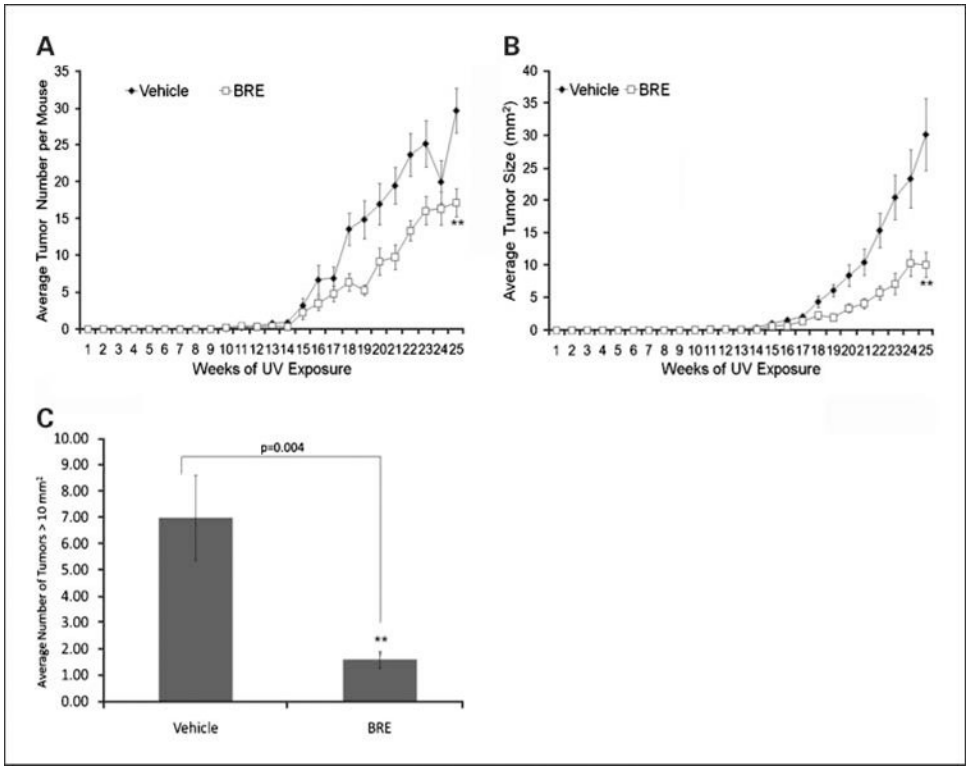


**Fig. 1.**

BRE significantly reduced UVB-induced carcinogenesis. Female SKH-1 mice ($n$ = 10/group) were treated with vehicle or BRE after exposure to 2,240 J/m$^2$ of UVB thrice weekly for 25 wks. Tumor measurements (number, length, and width) were taken beginning on week 11. BRE was able to significantly reduce tumor number (*A*) and tumor size (*B*; $P < 0.001$ and $P = 0.002$, respectively). *Points*, mean; *bars*, SD. *C*, BRE also significantly reduced the number of aggressive tumors ($P = 0.004$).

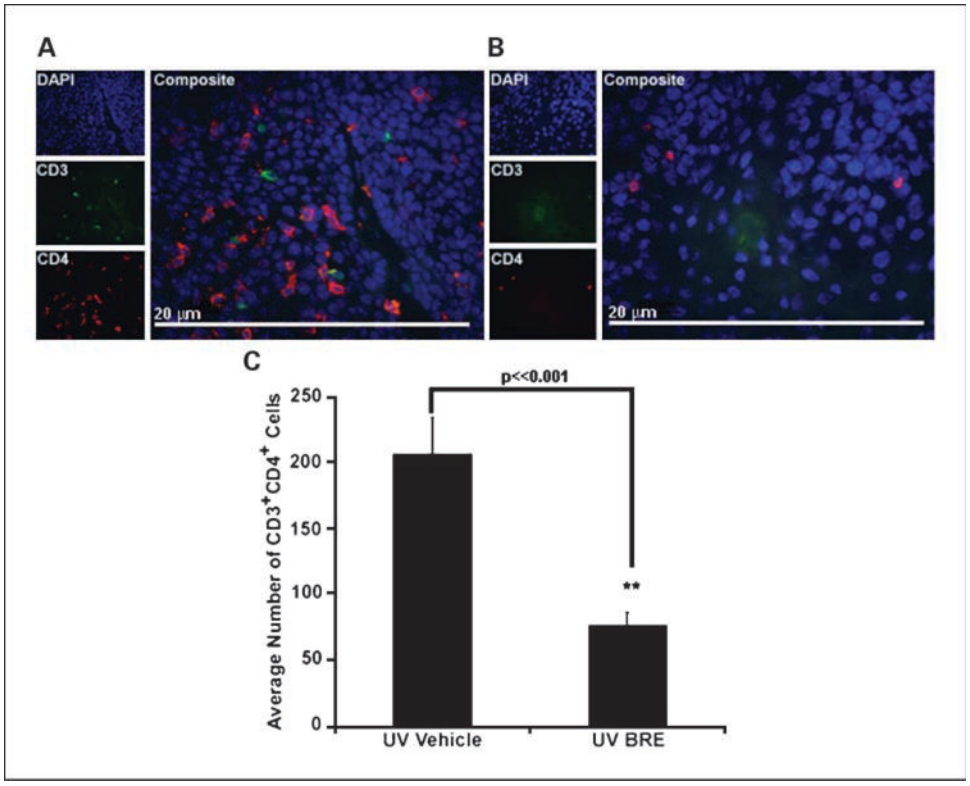


**Fig. 2.**

BRE altered tumor-infiltrating $CD4^+$ T-cell numbers. The number of $CD4^+$ T-cells infiltrating tumors of vehicle-treated mice (*A*) was significantly higher than BRE-treated mice (*B*). Magnification, ×600. Graphical representation of the data in *C* (**, $P \ll 0.001$). Columns, mean; bars, SE.

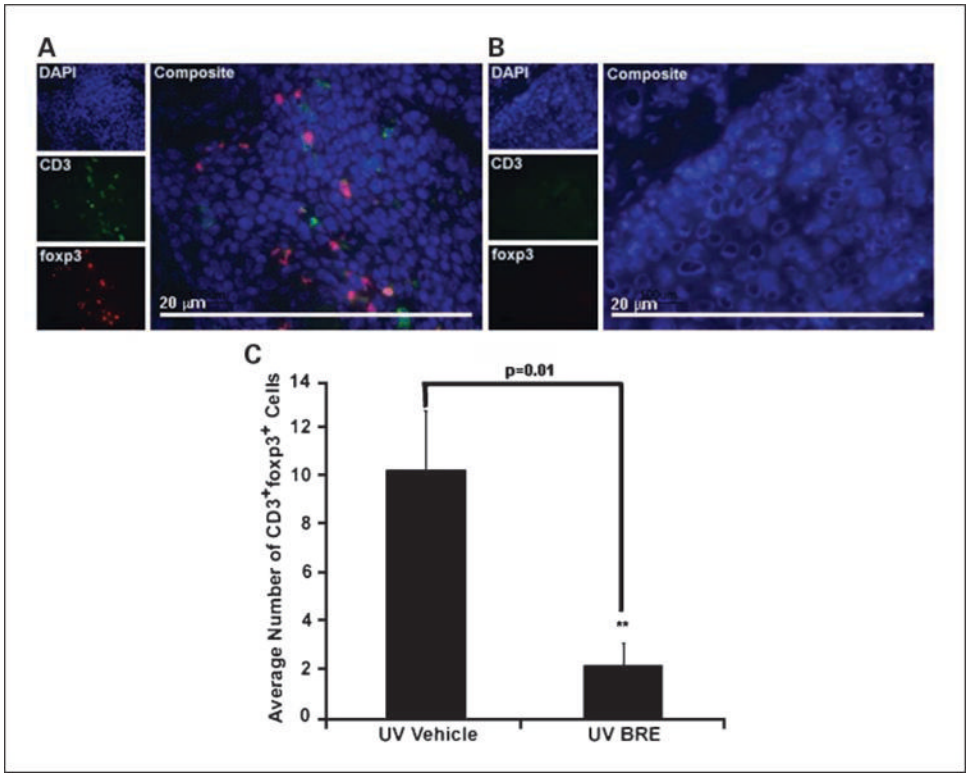


**Fig. 3.**

BRE altered tumor-infiltrating $CD3^+foxp3^+$ T-cell numbers. The number of $CD3^+foxp3^+$ T-cells infiltrating tumors of vehicle-treated mice (*A*) was significantly higher than BRE-treated mice (*B*). Magnification, ×600. Graphical representation of the data in *C* (**, $P = 0.01$). *Columns*, mean; *bars*, SE.

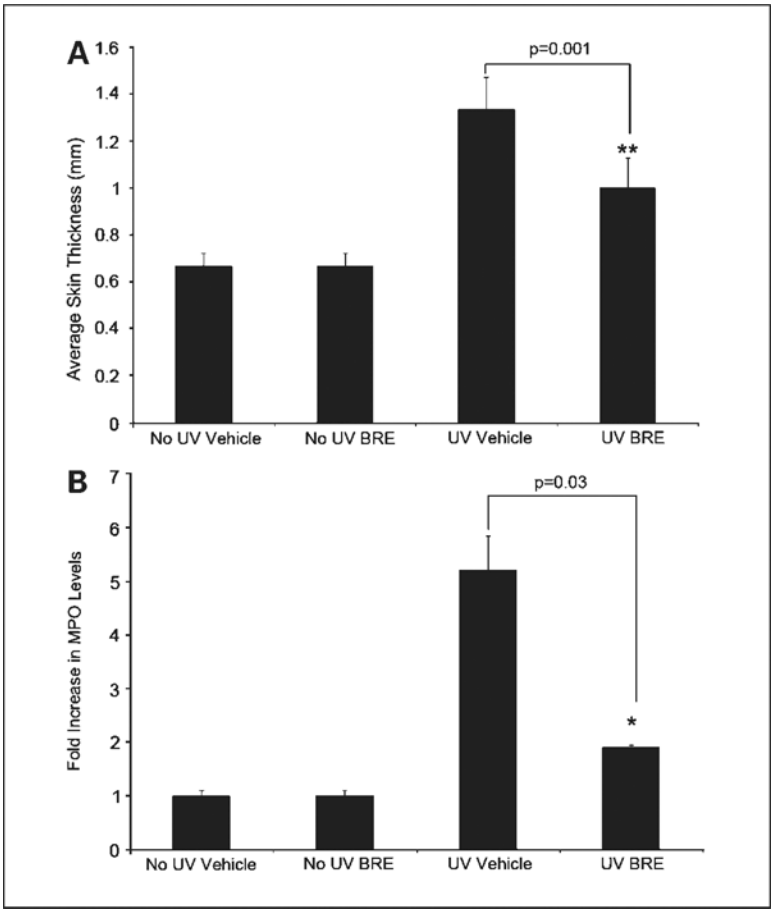


**Fig. 4.**

BRE significantly reduced UVB-induced edema and neutrophil activation. UVB induced edema as measured via single fold skin thickness was significant (**, $P = 0.001$), compared with UVB-exposed vehicle-treated controls (*A*). BRE significantly inhibited the UVB-induced increase in dorsal skin myeloperoxidase activity compared with vehicle (*, $P = 0.03$; *B*). *Columns*, mean fold increase of myeloperoxidase activity over matched no UV controls; *bars*, SD.

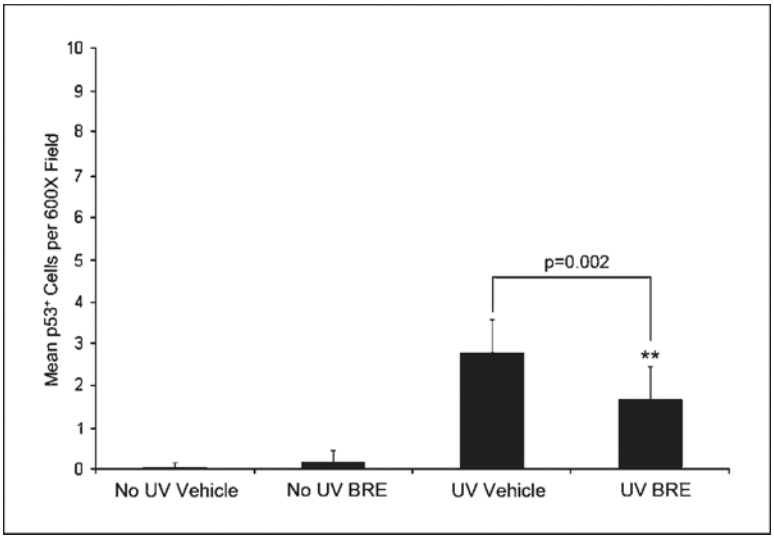


**Fig. 5.**

BRE reduced UVB-induced p53 expression. p53 was immuno histochemically localized and the number of positive cells was enumerated. *Columns*, average number of $p53^+$ cells per ×600 field; *bars*, SD (**, $P = 0.002$).

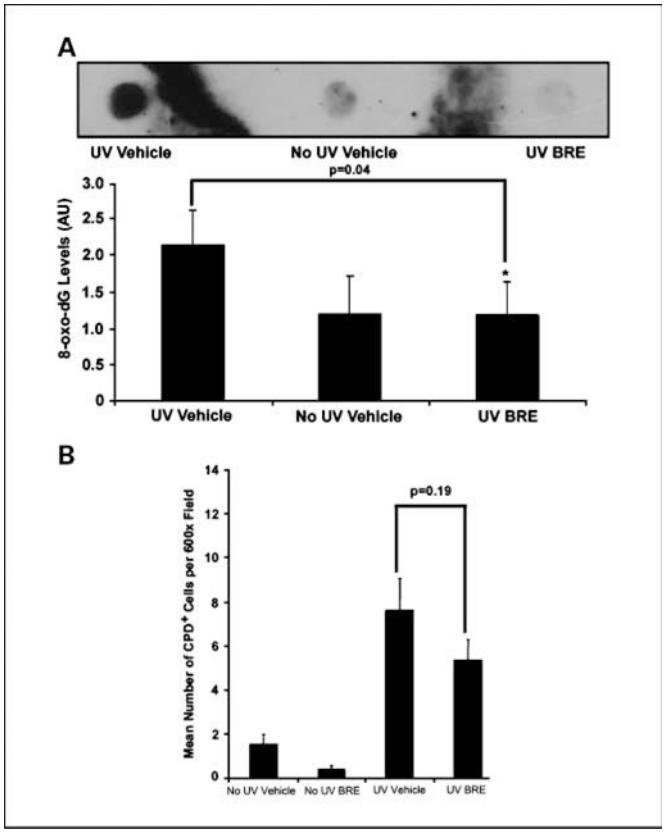


**Fig. 6.**

BRE reduced ROS-mediated DNA damage, but not direct DNA damage. After flash-freezing, DNA was isolated from epidermal scrapes and used in a Southwestern immunoblot (*A*). Densitometry was done using ImageJ. *Columns*, ratio of DNA to 8-oxo-dG (8-oxo-dG levels); *bars*, SD (*, $P = 0.04$; *B*). Paraffin sections were cut and stained for CPDs; keratinocytes staining positive were enumerated. *Columns*, mean number of CPD-positive cells per ×600; *bars*, SD (*C*).